Optics and Laser Technology 103 (2018) 109–117

Contents lists available at ScienceDirect

Optics and Laser Technology

journal homepage: www.elsevier.com/locate/optlastec

Full length article

Influence of Co^{2+} on electrical and optical behavior of Mn^{2+}-doped ZnS quantum dots

P. Sakthivel [a,*], S. Muthukumaran [b]

[a] PG & Research Department of Physics, H.H. The Rajah's College (Autonomous), Pudukkottai, Tamil Nadu 622 001, India
[b] PG & Research Department of Physics, Government Arts College, Melur, Tamil Nadu 625 106, India

ARTICLE INFO

Article history:
Received 30 May 2017
Received in revised form 27 October 2017
Accepted 4 January 2018

Keywords:
Co^{2+}-doped $Zn_{0.98}Mn_{0.02}S$ QDs
XRD
Photoluminescence
Dielectric constant
Electrical conductivity

ABSTRACT

Co^{2+}-doped $Zn_{0.98}Mn_{0.02}S$ quantum dots with various concentrations of Co^{2+} from 0% to 4% have been successfully synthesized by a simple co-precipitation method. X-ray diffraction (XRD) pattern confirmed the acquirement of cubic structure and phase purity in all the samples. The average crystallite size of the particles was ~3 nm observed from XRD result. Surface morphology of the samples was studied using scanning electron microscope (SEM). TEM study was also taken to know the structural parameters of the samples. Fourier transform infrared (FTIR) spectra proved the presence of Co^{2+} and Mn^{2+} in ZnS host lattice. Energy dispersive X-ray (EDX) analysis confirmed the elemental composition with their normal stoichiometric ratio. In the dielectric study, dielectric dispersion and dielectric loss were increased with Co^{2+} composition due to the increase of carrier concentration. From the AC conductivity measurement, the maximum conductivity was observed for Co^{2+} = 2% due to their higher charge carrier density and it was decreased for Co^{2+} = 4% due to the scattering of charge carriers. Because of the low dielectric constant at higher frequency, these materials can be used for high-frequency applications. The variation of peak intensity and wavelength shifting in UV-vis absorption and transmittance were discussed on the basis of formation of secondary phase and variation of charge carrier density. The continuous red shift of energy gap by Co^{2+}-doping is attributed to the direct energy transfer between excited states and 3d levels of Co^{2+} ions. Photoluminescence spectra showed the strong and broad blue emission bands between 468 nm and 483 nm. Since higher transmittance was observed for Co^{2+} = 2% addition, this material can be selected for optimum applications of optoelectronic devices.

1. Introduction

Nowadays synthesis of quantum dots (QDs) [1], especially QDs from the combinations of II - VI elements have been getting fascination due to their distinct impact of structural, morphological, optical, electrical and magnetic properties. ZnS is the first semiconductor [2] that can be selected as a best choice in this stream because of their large surface-volume ratio, wide band gap, large Bohr exciton radius, high exciton binding energy, distinct refractive index, and quantum confinement effect [3–7]. Doping of transition metals (TMS) with ZnS is carried out intentionally to modify their properties to extend the diverse applications including short-wavelength light emitting diodes, electro luminescence devices, flat panel displays, sensors, Laser diodes, solar cells, biological imaging, labelling and optoelectronic devices [8–13]. Incorporation of Mn^{2+} into ZnS host provides an enhancement in the luminescence efficiency and shortening the lifetime than its bulk form [14]. From our earlier attempt it was understood that Mn^{2+} = 2% doped ZnS QDs offers better optical and structural properties [15]. Since higher percent of Mn-doping produces secondary phase, it generates undesirable alterations in the properties. Dual-doping of TM with lower concentration is considered in the present investigation. TM such as Cu, Ni, Fe, Cr, Cd and Co was used as a dual-dopant in Mn:ZnS QDs due to their favourable and constructive progress in the structural, electrical, optical and magnetic properties [16–22].

Single crystals of Co^{2+}-doped zinc chalcogenides were prepared and its optical properties were studied comprehensively by Niu et al. [23]. Extensive emission of visible light was reported by Yang et al. [24] in Co^{3+} and Co^{2+}-doped ZnS nanoparticles. ZnS nanoparticles after co-doping with Co^{2+} and Cu^{2+} showed an enhancement in the photo luminescence emission [25]. Some of the researchers tried to prepare these dual doped nanoparticles in various methods [26–30]. The Doping of Mn^{2+} with ZnS provided better optical and

* Corresponding author at: Shanmuganathan Enginering College, Pudukkottai 622 507, Tamil Nadu, India.
E-mail address: sakthi1807@gmail.com (P. Sakthivel).

https://doi.org/10.1016/j.optlastec.2018.01.025
0030-3992/

photoluminescence properties and these were observed by many researcher. The doping of transition metal like Cobalt exhibited better structural and electrical properties. Mn^{2+}-doping gave possibility to tune for wide range of band gap of the material. The dual doping of Mn^{2+} and Co^{2+} may produce cumulative results in all aspects. Due to this intention to study the collective properties of ZnS dual doped by Mn^{2+} and Co^{2+}, we have attempted in the present work by using co-precipitation method. The structural, morphological, electrical, dielectric and optical properties have been studied and reported.

2. Preparation of $Zn_{0.98-x}Mn_{0.02}Co_xS$ (x = 0, 0.02, 0.04) QDs

Mn^{2+} and Co^{2+}-dual doped ZnS nanoparticles ($Zn_{0.98-x}Mn_{0.02}Co_xS$; x = 0, 0.02, 0.04) were synthesized by simple co-precipitation method at room temperature. Zinc acetate ($Zn(CH_3COO)_2.2H_2O$), sodium sulphide (Na_2S), manganese acetate ($Mn(CH_3COO)_2.2H_2O$) cobalt nitrate ($Co(No_3).6H_2O$ and aqueous ammonia solution were used for the preparation of the samples. All the analytical reagent grade chemicals were purchased from M/s. Merck with 99.99% purity. Hence further purification process was avoided.

The molar quantities were taken as per the targeted doping concentration i.e. (The doping composition of Mn^{2+} is fixed as 2% and Co^{2+} is varied from 0% to 4%) to prepare $Zn_{0.98-x}Mn_{0.02}$ Co_x S (x = 0, 0.02, 0.04) QDs. The source materials were weighed as per the expected compositions and were dissolved in 100 ml ultra-pure de-ionized water to make a 0.5 M solution. Separate solutions of manganese acetate, cobalt nitrate, zinc acetate and sodium sulfide were prepared. Sodium sulfide, Mn^{2+} and Co^{2+} solutions were added into zinc acetate solution drop wise and simultaneously under continuous stirring of 1000 rpm for 8 h at 60° C. The pH value of mixed chemical solution was standardised at 9.5 using ammonium solutions. A brownish precipitate was obtained at the end of the reaction. The final precipitate was filtered out and washed with de-ionized water and methanol to eliminate unwanted impurities during the synthesis steps. Finally, it was kept in micro-oven for 6 h at 65° C. The end compound was powdered evenly to get homogeneity in size. This process was repeated for getting Co^{2+} = 0%, 2% and 4% with Mn^{2+} (2%): ZnS QDs. A simple layout for the synthesis of nano particles using chemical method is illustrated in Fig. 1.

3. Characterization techniques

The crystal structure of $Zn_{0.98-x}Mn_{0.02}Co_xS$ (x = 0, 0.02, 0.04) QDs was determined by powder X-ray diffraction (XRD). Diffraction patterns were registered using Rigaku C/max-2500 diffractometer with the help of Cu Kα radiation at 40 kV and 30 mA. The study was performed from 2θ = 20° to 70° at the scan rate of 0.2°/min. High-resolution microstructural analysis was carried out using a scanning electron microscope (SEM, JEOLJSM 6390) and transmission electron microscopy (Philips- CM200) in the range of operating voltage as 20–200 kV. The study of surface morphology and the distribution of the particles in the sample were evidenced by SEM micrographs. The topological feature and composition of Zn2+, S, $Mn^{2+}$and Co^{2+} were determined by energy dispersive X-ray (EDX) using K and L lines. Dielectric and AC conductivity measurements were carried out in the frequency range from 50 Hz to 200 kHz using an LCR meter at room temperature. The samples used for this measurement were pelletized and their surfaces were coated with silver paste to form the structure of a parallel plate capacitor. To explore the optical behaviour of prepared samples, UV-visible optical absorption and transmittance studies were carried out using UV-visible spectrometer (Model: Lamda 35, Perkin Elmer) in the wavelength ranging from 300 mm to 600 mm at room temperature. The existence of chemical bonding was studied by Fourier Transform infrared (FTIR) spectrometer (Model: Perkin Elmer, Make: Spectrum RXI) from wave number 400 to 4000 cm^{-1}. The samples used for this study were taken in the form of pellets prepared by mixing the nanoparticles with KBr at 1 wt%. PL study was taken using wavelength of 325 nm as excitation energy (Hitachi F-2500) to record the radiative recombination process. All the studies were taken at room temperature.

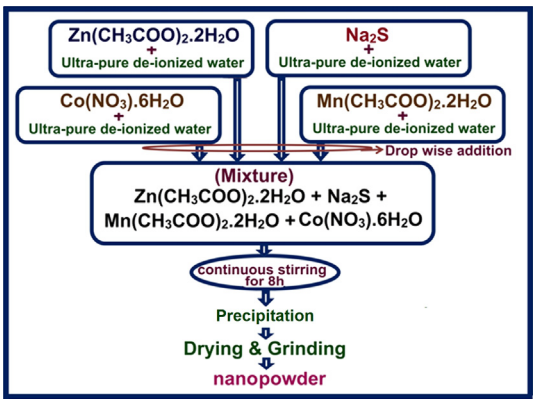

Fig. 1. Flow chart diagram for preparation of $Zn_{0.98-x}Mn_{0.02}Co_xS$ (x = 0, 0.02, 0.04) QDs.

4. Results and discussion

4.1. X-ray diffraction: structural studies

XRD patterns were taken from 20° to 70°, and these results were used to investigate the effect of Mn^{2+} and Co^{2+} doping on the structure and the phase composition of ZnS structure. The typical XRD patterns of the Mn^{2+} doped and (Mn^{2+}, Co^{2+}) dual-doped ZnS QDs synthesized by co-precipitation method are shown in Fig. 2a. From this figure, It has been observed that the XRD patterns are broadened with three main peaks corresponding to the (1 1 1), (2 2 0) and (3 1 1) planes. The major peaks matched closely with the JCPDS card No. (05-0566). All the peaks in the XRD patterns clearly indicated that the samples possess a cubic structure. In the XRD pattern, no obvious evidence was observed in the form of strange elements or other impurities. Results indicated that all the samples were in pure phase and the entry of Mn^{2+} and Co^{2+} not altered the original cubic structure. As shown in Fig. 2a, the bandwidth of the XRD peaks corresponding to (1 1 1) plane is broadened at high Co^{2+} concentration due to the crystalline nature of the nano-particles.

The variation of peak intensity and peak position (2θ) for different Co^{2+} concentration is shown in Fig. 2a. The peak position along (1 1 1) is gradually shifted towards higher 2θ degree side when Co^{2+} incorporation is increased from 0% to 4% and this is attributed to the lesser ionic radius of Co^{2+} (0.72 Å) than Zn^{2+} (0.74 Å) [26,30]. Peak intensity for (1 1 1) plane increased around threefold when the addition of Co^{2+} (Co^{2+} = 2%) and slightly decreased for further addition of Co^{2+} (Co^{2+} = 4%). The average crystallite size is determined by using the Debye-Scherrer's formula [31],

$$Average\ crystallite\ size\ (D) = \frac{0.9\lambda}{\beta \cos\theta} \quad (1)$$

where λ is the wavelength of X-ray used, β is the full-width at half-maximum (FWHM) intensity of the diffraction peak along (1 1 1) plane and θ is the angle of the Bragg's diffraction. The